Researches in Earth Sciences

Journal homepage: https://esrj.sbu.ac.ir

Research Article

Integrated remote sensing analysis of snow cover and topographic influences in mountainous regions (Case study: Marivan County, Iran)

Batool Zeinali[1*], Sina Khonkham[1], Sayyad Asghari Saraskanroud[1]

1-Department of Physical Geography, Faculty of Social Sciences, University of Mohaghegh Ardabili, Ardabil, Iran

Received: 01 Jul 2025 Accepted: 06 Sep 2025

Abstract

Snow plays a vital role in the hydrological cycle, especially in mountainous regions, significantly affecting water resources, agriculture, and natural hazard mitigation. This study employs remote sensing data to analyze the spatiotemporal distribution of snow cover and its relationship with precipitation and topographic variables, including slope, aspect, and elevation in Marivan County, western Iran. Sentinel-2 and Landsat satellite imagery from snow cover seasons between 2021 to 2024, alongside several snow indices (NDSI, NDSII, NDSInw, S3, SWI and NBSI-MS), were used to generate snow cover maps. Satellite-based precipitation datasets (CHIRPS and PERSIANN) were utilized to explore correlation between snow cover and precipitation patterns. Results indicated that the S3 and SWI indices provided the highest accuracy in snow detection, with Sentinel-2 imagery outperforming Landsat due to its finer spatial resolution. Topographic analysis revealed that regions with higher elevation, northern aspect and gentle slopes had the densest snow cover. Overall, this study highlights that effectiveness of intergrating optical remote sensing, precipitation data, and topographic information for accurate monitoring of snow cover in mountainous areas.

Keywords: Snow Mapping, Topographic variables, Sentinel-2, Landsat, Spectral Indices.

Citation: Zeinali, B. et al, 2025. Integrated remote sensing analysis of snow cover, *Res. Earth. Sci:* 16(Special Issue), (182-192) DOI: 10.48308/esrj.2025.240523.1283

* Corresponding author E-mail address: zeynali.b@uma.ac.ir

Introduction

Background

Snow is one of the most vital forms of precipitation in mountainous regions and plays a central role in the hydrological cycle. It provides water for irrigation, drinking supply, and hydropower production. In low-water seasons, snow acts as a natural reservoir, gradually releasing water. However, rapid snowmelt during intense spring rainfall trigger destructive floods, threatening both infrastructure and water security (Tekeli et al, 2005). The spatial distribution of snow is highly uneven due to terrain complexity. Ground-based measurements, such as snow gauges, offer reliable data but are limited in coverage especially in remote or rugged areas (Yarahmadi et al, 2022). Field surveys are also costly and labor-intensive. Satellite remote sensing therefore provides a practical alternative for large-scale monitoring (Abdollahi et al, 2017). Optical sensors, sensitive to snow reflectance, have been widely used to map snow cover. While precipitation products such as CHIRPS and PERSIANN enhance monitoring by combining spatial coverage with high temporal resolution. (Xie and Xiong, 2011). Climate change is expected to substantially reduce snow extent and shorten the duration of snow cover worldwide (Mitterwallner et al, 2024). This decline poses significant risks for regions that depend on snowmelt as a primary water source. Reduced snow reliability affects agriculture, energy production, tourism, and flood management (Willibald et al, 2020). In high-altitude environments, changes in snowpack also influence avalanche hazards, ecological stability, and biodiversity (Ortner et al, 2023). Overall, the trend points to a widespread reduction in snow resources with major hydrological and socio-economic consequences. These challenges highlight the urgent need for accurate, multi-source snow monitoring systems. In mountainous areas such as western Iran, where water availability and agricultural productivity are closely tied to seasonal snow cover, integrating satellite observations with climatic and topographic data is essential. This study aims to address this gap by assessing snow cover variability and its relationship with topographic parameters, providing insights for future water management under changing climate conditions.

Literature review

Several studies have demonstrated the effectiveness of satellite imagery and spectral indices for snow cover detection. Liu et al. (2021) used MODIS data to study snow cover changes in the Karakoram Mountains and observed significant declines, especially in the southern and eastern regions, correlating with temperature and precipitation trends. Yan et al. (2020) introduced new indices—NDWINS and NDSINW—using Landsat sensors for improved identification of water and snow bodies on the Tibetan Plateau. Varade and Dikshit (2018) applied Sentinel-2 data and indices such as NDSI and S3 to estimate snow moisture content in the Himalayas, achieving an RMSE of 0.07. Similarly, Asghari and Modirzadeh (2019) employed Sentinel-2 MSI imagery and indices like NDSI, S3, and NDWI to map snow cover in Ardabil and Sarein cities, validating their results with ground observations and achieving over 91% overall accuracy. These findings confirm the strong performance of remote sensing methods for snow monitoring in mountainous areas. Given the increasing concern about water resources under climate change, snow cover has become a critical focus, particularly in arid and semi-arid countries like Iran, where mountainous regions such as Kurdistan serve as major water reservoirs.

Scope and objective

This study focuses on Marivan County in western Iran, a predominantly mountainous region within the Zagros range and an important snow-accumulating area. The research aims to analyze the spatial distribution of snow cover and evaluate its relationship with topographic factors (elevation, slope, and aspect) as well as precipitation patterns during the winter seasons from 2021 to 2024.

The specific objectives of the study are to:

- Generate snow cover maps using Sentinel-2 and Landsat imagery.
- Apply and compare six spectral snow indices (NDSI, NDSII, NDSI_nw, S3, SWI, and NBSI-MS).
- Integrate satellite-based precipitation dataset (CHIRPS and PERSIANN) with snow cover maps.
- Evaluate the influence of topographic parameters on snow accumulation and persistence.

- Identify high snow-density zones based on terrain characteristics to support water resource planning and hazard management.

The selection of snow indices in this study is based on their proven performance in previous research, their spectral sensitivity to snow characteristics, and their ability to reduce misclassification with other land cover types such as clouds and water. For instance, NDSII-1 and NDSI_nw are enhansed versions of the traditional NDSI, designed to minimize errors by excluding shortwave water-absorbing bands. Indices such as S3 and SWI incorporate near-infrared and SWIR bands to improve snow moisture detection, while NBSI-MS is tailored to distinguish snow from heterogeneous surfaces like vegetation or mixed pixels. In contrast, methods such as MODSCAG rely on spectral unmixing and are specifically designed for MODIS data with coarser resolution, making them less suitable for Sentinel-2 or Landsat-based high-resolution snow mapping. Therefore, the indices selected in this study provide an optimal balance between spectral accuracy and spatial resolution, ensuring a robust framework for snow monitoring in mountainous terrain.

Materials and Methods

Study area

Marivan city, located in Kurdistan province in western Iran and near the Iran-Iraq border, covers area of more than 2336 km^2. It lies at latitude "35°00'3" N and longitude "00'45'46" E, (Figure 1). The region is characterized by divers topography and forests which contribute to its ecological and environmental significance. Marivan's varied elevation and mountainous terrain strongly influence its local climate, with abundant seasonal precipitation and substantial water resources. Major rivers, springs, and lakes- including the near Zarivar Lake-supply the region with considerable surface water. Beyond its environmental importance, Marivan also holds strategic value for scientific research. Its geographical location, complex topography and climatic variability make it an ideal site for investigating water resources, climate change, and snow cover dynamics. The average elevation of the city is about 1320 meters above sea level.

Data set used

Snow Cover Data

Satellite images from the winter months (December to March) over three years were used to investigate the snow cover in the study area. The data used include Landsat OLI / TIRS and Sentinel-2 MSI satellite images. These satellites were selected due to their suitable temporal coverage, acceptable spatial resolution, and easy access to data. Landsat images with a spatial resolution of 30 m and Sentinel-2 with a spatial resolution of 10 m in the visible and near-infrared (NIR) bands allow for accurate identification and monitoring of snow cover, as seen in Table 1 for the dates of the images used.

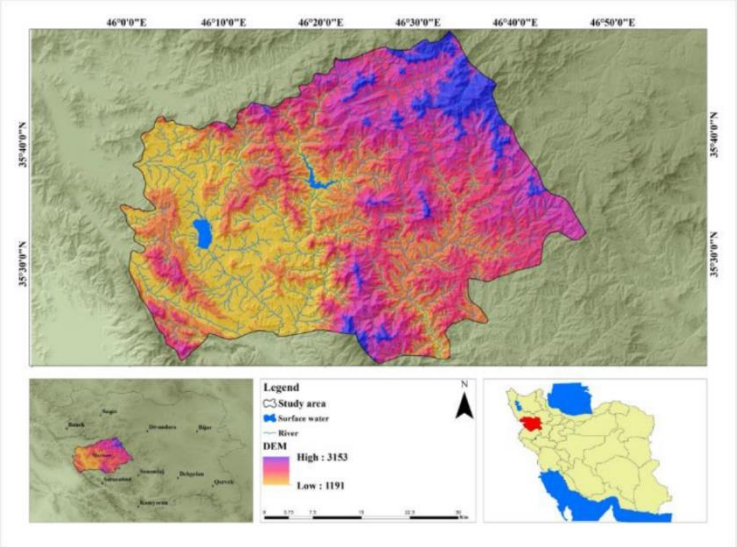

Fig. 1: Location map of the study area

Table 1: Landsat 8 and Sentinel-2 satellite images used in this research along with spectral characteristics and cloud cover (2024-2021)

Sensor	Acquisition Date	Spectral Band with Wavelet (µm)	Cloud Cover
Sentinel-2	19 December 2021	Costal (0.443)	2.4%
	8 January 2022	Blue (0.490)	0.0%
	7 February 2022	Green (0.560)	0.5%
	14 March 2022	Red (0.665)	2.2%
	19 December 2022	Vegetation red edge (0.705)	0.0%
	3 January 2023	Vegetation red edge (0.740)	3.4%
	17 February 2023	Vegetation red edge (0.783)	4.2%
	22 March 2023	NIR (0.842)	0.0%
	4 December 2023	Vegetation red edge (0.865)	0.02%
	18 January 2024	SWIR-Cirrus (1.375)	0.09%
	12 February 2024	SWIR-1 (1.610)	0.0%
	13 March 2024	SWIR-2 (2.190)	0.0%
Landsat 8	7 December 2021		11.11%
	8 January 2022		2.21%
	1 February 2022	Costal (0.43–0.45)	19.57%
	13 March 2022	Blue (0.45–0.51)	25.03%
	18 December 2022	Green (0.53–0.59)	2.76%
	3 January 2023	Red (0.63–0.67)	1.56%
	4 February 2023	NIR (0.85–0.88)	18.28%
	28 March 2023	SWIR-1 (1.57–1.65)	3.53%
	5 December 2023	SWIR-2 (2.11–2.29)	0.70%
	6 January 2024	Cirrus cloud (1.36–1.38)	20.37%
	7 February 2024		44.58%
	2 March 2024		22.86%

To extract snow cover maps, the spectral indices NDSI, NDSII-1, S3, SWI, NDSI_nw, and NBSI-MS were used, which are widely used in snow identification, and you can see information about the indices in Table 2. Also, in Figure 2, you can see a diagram of how to extract snow surface from Sentinel-2 and Landsat images.

Table 2: Snow cover measurement indicators

Name	Index	Threshold	References
Normalized Difference Snow Index	NDSI	0.4<	(Nagler et al, 2016)
Normalized Difference Snow Index II - Version 1	NDSII-1	0.4<	(Dixit et al, 2019)
Normalized Difference Index with No Water Information	NDSI_nw	0.4<	(Yan et al, 2020)
Snow Index 3	S3	0.18<	(Nagler et al, 2016)
Snow Water Index	SWI	0.21<	(Dixit et al, 2019; Hall et al, 1995)
Non-Binary Snow Index for Multi-Component Surfaces	NBSI-MS	-1<	(Arreola-Esquivel et al, 2021)

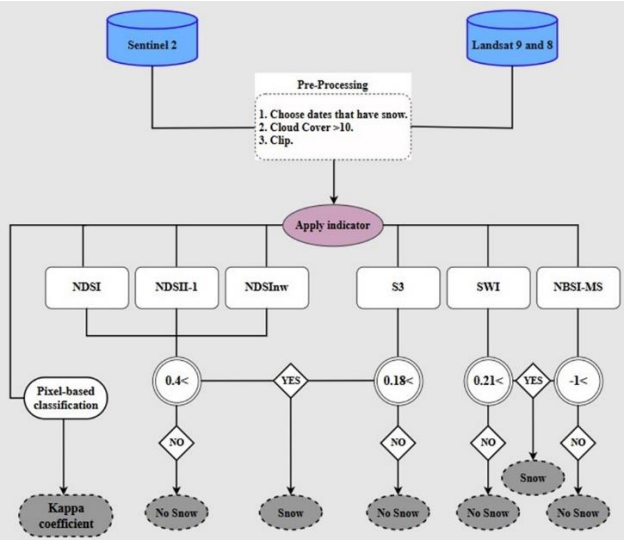

Fig. 2: The data layers used in this study, a: elevation, b: slope, c: aspect, d: Rainfall

Meteorological Data

In this study, in addition to using Landsat and Sentinel satellite images to extract snow cover, precipitation data from two satellite products, CHIRPS and PERSIANN, were also used for the same three-year period of the winter season. Technical information related to the bands and characteristics of both satellite products is presented in Table 3. CHIRPS (Climate Hazards Group InfraRed Precipitation with Station data) data, combining station data and infrared satellite images, provides broad spatial coverage and daily temporal resolution and is considered a reliable source in climate studies. In contrast, PERSIAN (Precipitation Estimation from Remotely Sensed Information using Artificial Neural Networks) data, which are developed based on artificial neural networks, use a combination of infrared and microwave data to estimate precipitation and provide access to precipitation data with hourly temporal resolution.

Table 3: Spatial and temporal characteristics of PERSIANN-CDR and CHIRPS satellite precipitation data

Name	Units	Pixel Size	Bands	Cadence	resolution (grade)
PERSIANN-CDR	mm	27830 meters	precipitation	1 Day	0.25
CHIRPS	mm/d	5566 meters	precipitation	1 Day	0.05

This study extracted CHIRPS and PERSIANN data from the Google Earth Engine (GEE) database. After performing regional slicing, spatial scaling, and temporal aggregation, the data were converted into a standard format comparable to each other and to ground data. Finally, the temporal trend of precipitation during the study period and its relationship with snow cover changes were analyzed and evaluated. To evaluate the accuracy of satellite-based precipitation datasets (CHIRPS and PERSIANN) against ground station observations, three statistical metrics were employed: Root Mean Square Error (RMSE), Mean Absolute Error (MAE), and Pearson correlation coefficient (r). The statistical significance of correlation coefficients was tested at the 95% confidence level ($p < 0.05$).. These metrics allow for a quantitative assessment of the difference and correlation between satellite-derived precipitation and ground-based records.

Topographic data

In order to investigate the effect of topographic features on the spatial distribution of snow cover, a Digital Elevation Model with a spatial resolution of 12.5 m was used in this study. This model, which was obtained from high-precision ALOS PALSAR satellite data, allows for a more accurate analysis of geomorphological variables at a local scale. This model extracted three layers, height, slope, and aspect, which are considered the most important effective parameters in the snow accumulation and melting pattern. The slope direction, especially in mountainous areas, is important in the amount of solar radiation received and affects snow's stability or faster melting. Also, steeper slopes are more prone to runoff and snow slides, while gentler slopes have a greater potential to maintain snow cover during cold periods. All topographic layers were generated and analyzed co-locally with snow cover, precipitation, and other environmental indicators. This data fusion investigated the relationship between terrain characteristics and the spatiotemporal snow cover distribution in the study area.

Results and Discussion

This study evaluated various remote sensing indices for snow cover identification. The results showed that the indices can distinguish snow areas from other land surface covers. However, their accuracy varies depending on regional conditions and spectral characteristics. Due to this study's large number of images and indices, we only show examples of the output maps. Figures 3 to 6 show that these indices' output provides accurate snow cover distribution maps and allows for favorable visual interpretation. Despite the general ability of all the indices considered in snow cover identification, their accuracy is affected by the index value and input data type. Figures 3 and 4 show an example of a snow map extracted from Sentinel-2 images. Figures 5 and 6 show snow maps obtained from Landsat data, clearly demonstrating the difference in accuracy and resolution between these two data sources.

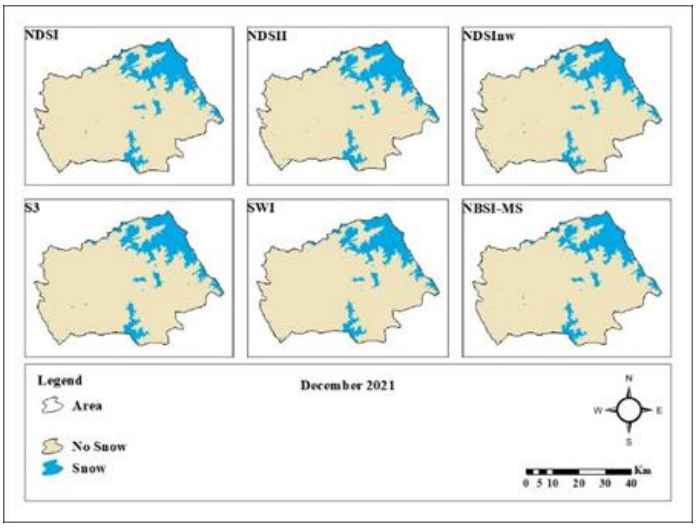

Fig. 3: Sample snow cover map extracted using different remote sensing indices for December 2021 (Sentinel-2)

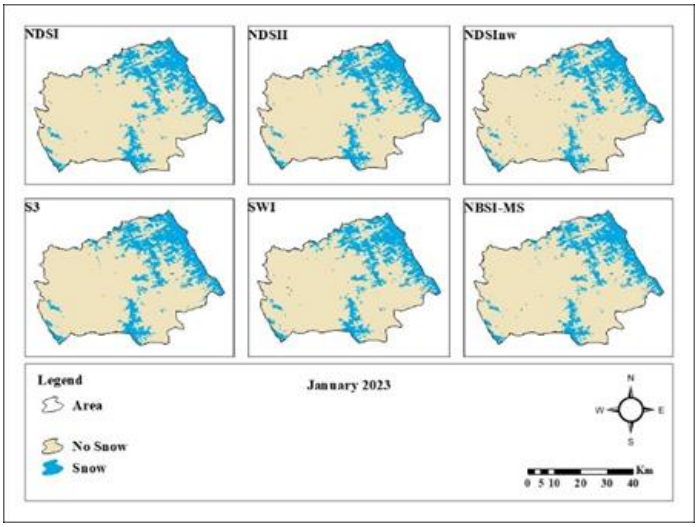

Fig. 4: Sample snow cover map extracted using different remote sensing indices for January 2023 (Sentinel-2)

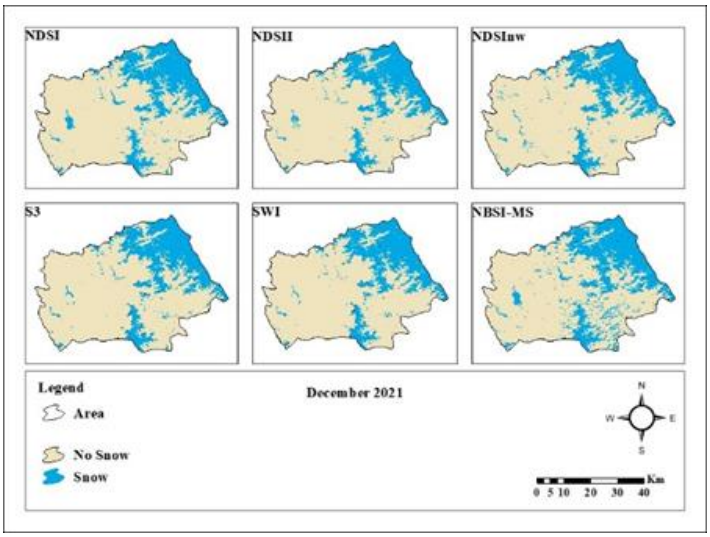

Fig. 5: Sample snow cover map extracted using different remote sensing indices for December 2021 (Landsat)

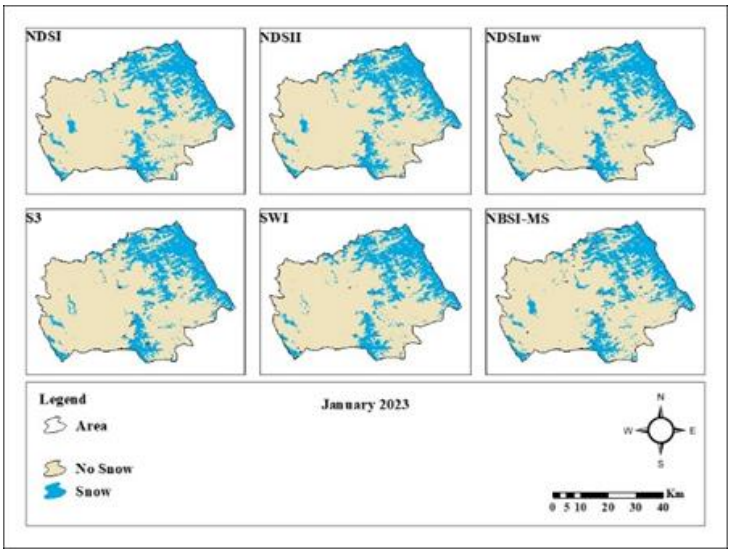

Fig. 6: Sample snow cover map extracted using different remote sensing indices for January 2023 (Landsat)

Based on the kappa coefficient values in Tables 4 and 5 for Landsat and Sentinel-2 satellite data, respectively, Sentinel-2 images have provided more accurate results than Landsat due to their higher spatial resolution. In Sentinel-2 data, the S3 index with a kappa coefficient of 0.96763 has the highest accuracy, and the NBSI-MS index with a value of 0.93543 has the lowest accuracy. In contrast, the SWI index with a value of 0.9538 in Landsat images showed the best performance, while NBSI-MS recorded the lowest accuracy with 0.7668. In general, spectral indices have performed reasonably well in extracting snow areas. However, in mountainous areas, factors such as shadow and topographic features can reduce the accuracy of the results. The overall comparison of the average kappa coefficient between the two satellites also showed that Sentinel-2, with a value of 0.955985, performs better than Landsat, with a value of 0.88211, indicating the higher accuracy of the indicators applied in Sentinel-2. This research showed that the selected indices perform well in identifying snow areas and can be an effective alternative to traditional classification methods. The exact values of the kappa coefficient for all the indices analyzed are presented in Tables 4 and 5, which allows for a precise comparison of the performance of each index.

Table 4: Accuracy of snow index based on Kappa coefficient in Sentinel-2 images during the period of 2021 to 2024

TIME	NDSI	NDSII	NDSI_nw	S3	SWI	NBSI-MS
2021-12-19	0.9627	0.9652	0.9335	0.9724	0.9589	0.9256
2022-01-08	0.9046	0.9835	0.9927	0.9814	0.9843	0.9277
2022-02-07	0.8921	0.9107	0.9729	0.8889	0.9267	0.9749
2022-03-14	0.9859	0.9770	0.9841	0.9727	0.9848	0.9782
2022-12-19	0.9883	0.9827	0.8907	0.9907	0.9758	0.8861
2023-01-03	0.9943	0.9892	0.8503	0.9953	0.9836	0.8295
2023-02-17	0.9971	0.9947	0.9976	0.9916	0.9962	0.9979
2023-02-22	0.9877	0.9878	0.9857	0.9870	0.9876	0.9856
2023-12-04	0.9816	0.9792	0.8951	0.9871	0.9719	0.9317
2024-01-18	0.9204	0.9200	0.8928	0.9302	0.9160	0.8900
2024-02-12	0.9247	0.9271	0.9110	0.9355	0.9231	0.9181
2024-03-13	0.9806	0.9803	0.9810	0.9788	0.9806	0.9799

Table 5: Accuracy of snow index based on Kappa coefficient in Landsat images during the period of 2021 to 2024

TIME	NDSI	NDSII	NDSI_nw	S3	SWI	NBSI-MS
2021-12-07	0.9008	0.9823	0.9981	0.9722	0.9967	0.8943
2022-01-08	0.6713	0.8281	0.9790	0.9721	0.9746	0.6511
2022-02-01	0.6756	0.6784	0.9297	0.4333	0.9329	0.9861
2022-03-13	0.8712	0.9468	0.9945	0.9539	0.9991	0.8444
2022-12-18	0.8305	0.9741	0.8879	0.9598	0.9721	0.6895
2023-01-03	0.7963	0.8951	0.9821	0.9224	0.9742	0.7707
2023-02-04	0.9253	0.8935	0.8256	0.8883	0.9140	0.7563
2023-02-28	0.9639	0.9813	0.9903	0.9652	0.9894	0.9652
2023-12-05	0.6654	0.8273	0.8120	0.8434	0.8308	0.5205

2024-01-06	0.8738	0.8922	0.8713	0.9131	0.8809	0.5531
2024-02-07	0.9873	0.9870	0.9481	0.9896	0.9847	0.9077
2024-03-02	0.7926	0.9970	0.9981	0.9987	0.9970	0.6630

Figures 7 and 8 show the snow area using Landsat and Sentinel-2 satellite data and indices such as NDSI, NDSI-I, NDSI_nw, S3, SWI and NBSI-MS, respectively. The lowest snow cover was recorded in December 2023, and the highest in February 2023 (more than 2000 km2). Snow cover increases in winter and decreases in summer due to natural melting. S3 in Sentinel-2 and SWI in Landsat are the most accurate indices, and the accuracy of the indices is directly related to the extracted snow area. The slight differences between the methods and the influence of environmental factors indicate the importance of precision in preprocessing and the use of these methods for monitoring snow cover in different regions.

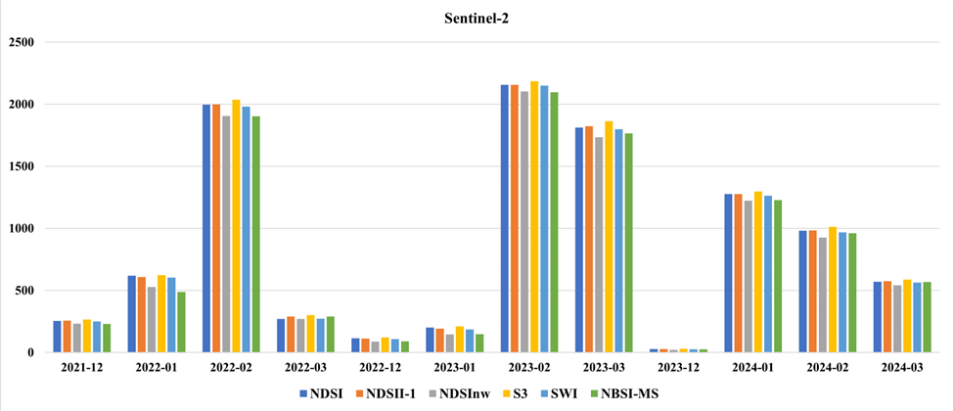

Fig. 7: Area diagram of snowy areas (Sentinel-2)

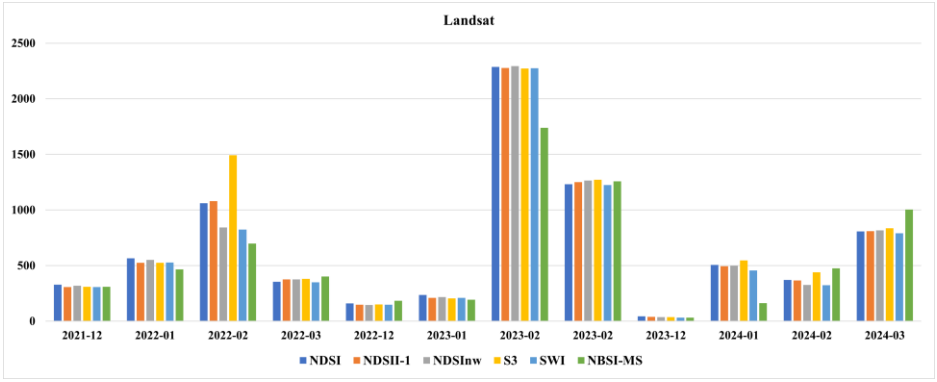

Fig. 8: Area diagram of snowy areas (Landsat)

The study analyzed monthly precipitation data from December 2021 to March 2024 using the CHIRPS and PERSIANN ground stations (Figure 9). The results showed that there are differences between these sources. For example, in March 2023, the ground station recorded 174.2 mm of precipitation, CHIRPS 172.836 mm, and PERSIANN 119.973 mm. However, all sources showed a similar seasonal pattern: precipitation is higher in winter (January, February and March). To quantitatively evaluate the agreement between satellite-based precipitation data (CHIRPS and PERSIANN) and ground station observations, statistical metrics including RMSE, MAE, and r were calculated. The results showed that CHIRPS data had lower error values (RMSE = 92.63 mm, MAE = 64.13 mm), while PERSIANN showed a higher correlation with ground station data ($r = 0.40$, $p < 0.05$), indicating that the correlation is statistically significant at the 95% confidence level. These findings highlight that although both datasets present general seasonal trends, their accuracy varies and validation with ground observations remains essential for reliable hydrological applications. Comparison with ground station data showed that CHIRPS and PERSIANN are sometimes more accurate, but validation with ground data is necessary. The precipitation data

are correlated with snow-cover surface images from Landsat and Sentinel-2. Heavy winter precipitation, such as in February 2023, increased the snow area to over 2,000 km^2, while low precipitation (e.g., December 2022) has decreased snow cover. Seasonal patterns and differences in measurement methods highlight the importance of accurate and simultaneous data analysis to visualize environmental changes better.

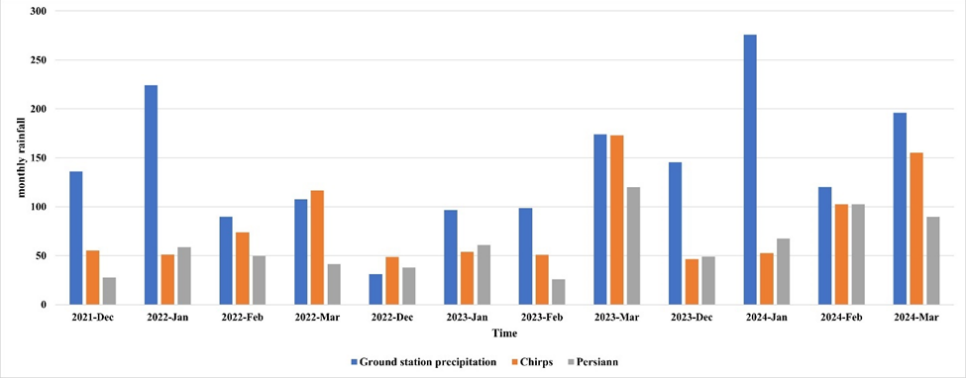

Fig. 9: Seasonal changes of precipitation in the period 2021-2024: comparison of ground station data, CHIRPS and PERSIANN

In order to more accurately examine the effect of topographic factors on the spatial distribution of snow cover, maps of slope, slope direction, and elevation of the study area were combined and analyzed with snow cover maps and precipitation data. Figures 10 and 11 show the study area's slope and slope direction maps. These analyses showed that slope direction plays an important role in snow persistence and accumulation; the highest snow density was observed in the northern and northeastern directions. These directions in the Northern Hemisphere usually receive less solar radiation, which reduces the melting rate and increases snow persistence. Also, analysis of the slope map showed that areas with gentle to moderate slopes (about 5 to 20%) had the highest snow cover. In contrast, snow accumulation was lower in areas with very steep slopes due to increased runoff velocity and high probability of snow slides. The study of the elevation pattern also showed that areas with an altitude of more than 1700 meters above sea level have significantly more extensive snow cover. The lower temperatures and higher precipitation at higher altitudes can explain this relationship. Also, by spatial comparison of CHIRPS and PERSIANN satellite precipitation maps with elevation and slope direction layers, it was found that high-altitude areas with northern slopes, in addition to high snow cover, also received more precipitation, which confirms the positive relationship between precipitation and snow accumulation in these areas.

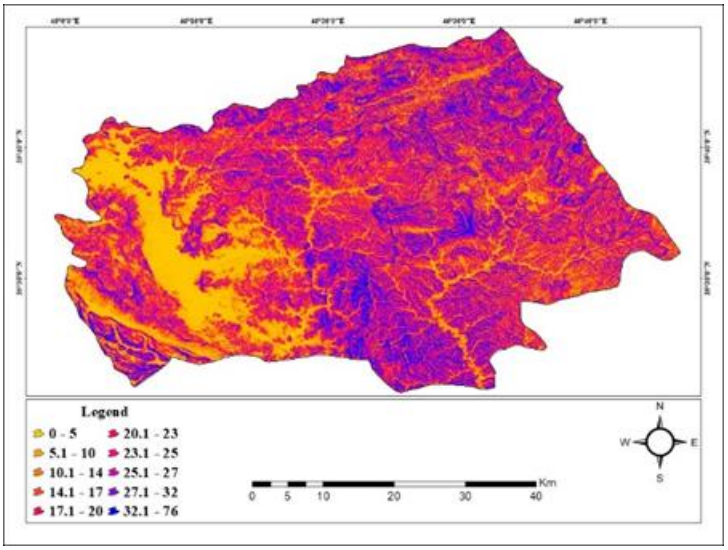

Fig. 10: Aspect Classification Map of Marivan County Derived from DEM Data

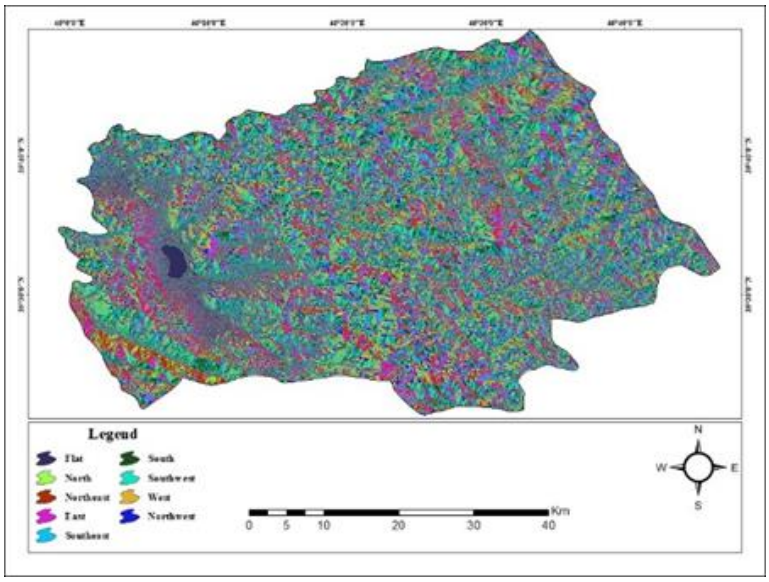

Fig. 11: Slope Classification Map of Marivan County Derived from DEM Data

However, factors such as shadow, vegetation, cloud cover, and similar spectral features of some phenomena may interfere with the accuracy of snow cover maps. Also, the accuracy of the indices may vary depending on local and temporal conditions.

Conclusion

This study evaluated snow cover in Marivan County during the winters of 2021 to 2024 using Sentinel-2 and Landsat imagery combined with spectral indices such as NDSI, NDSII, NDSI_nw, S3, SWI, and NBSI-MS. The results showed that all indices performed reasonably well, with the S3 index in Sentinel-2 and SWI in Landsat providing the highest accuracy. Analysis of CHIRPS and PERSIANN precipitation datasets revealed a strong correspondence with the spatial and temporal patterns of snow cover, confirming their potential as reliable alternatives to ground-based observations. Topographic factors-including elevation, slope and aspect-were also found to strongly influence snow distribution. In particular, high-elevation zones with gentle slopes and north-facing aspects exhibited the greatest snow accumulation, underlining the importance of geomorphology in snow studies. The integration of optical satellite imagery, precipitation data, and topographic information proved effective for snow monitoring in mountainous regions. Such an approach offers valuable applications for water resource management, flood risk assessment, and drought forecasting. Nevertheless, limitations such as cloud cover in optical images and the coarse resolution of DEM data may affect snow detection accuracy, especially in complex terrain. Future works should incorporate higher-resolution DEMs, cloud-penetrating sensors (e.g., SAR) and machine learning algorithms to further improve snow cover mapping.

Acknowledgment

There has been no support from any organization to carry out this project.

References

Abdollahi, A., Jahani, A., Rayegani, B. and Mohammadi Fazel, A., 2017. Impact assessment of dam construction on land use changes in the western and southern catchments of Lake Urmia using satellite images, Environmental Researches, v. 8(15), p. 39-50.

Arreola-Esquivel, M., Toxqui-Quitl, C., Delgadillo-Herrera, M., Padilla-Vivanco, A., Ortega-Mendoza, G. and Carbone, A., 2021. Non-binary snow index for multi-component surfaces. Remote Sensing, v. 13(14), https://doi.org/10.3390/rs13142777.

Asghari Saraskanroud, S., Molanouri, E., Safari, S. and Ghale, E., 2021. Evaluation of the performance of snow and water spectral indices for the separation of water and snow/ice cover (SCG) features. Physical Geography Quarterly, v. 14(53), p. 135-152.

Collischonn, B., Collischonn, W. and Tucci, C.E.M., 2008. Daily hydrological modeling in the Amazon basin using TRMM rainfall estimates. Journal of Hydrology, v. 360(1-4), p. 207-216.

Dixit, A., Goswami, A. and Jain, S., 2019. Development and evaluation of a new “Snow

Water Index (SWI)" for accurate snow cover delineation. Remote Sensing, v. 11(23), https://doi.org/10.3390/rs11232774.

Duan, Z. and Bastiaanssen, W., 2013. First results from Version 7 TRMM 3B43 precipitation product in combination with a new downscaling–calibration procedure. Remote sensing of Environment, v. 131, p. 1-13.

Ghajarnia, N., Liaghat, A. and Arasteh, P.D., 2015. Comparison and evaluation of high resolution precipitation estimation products in Urmia Basin-Iran. Atmospheric Research, v. 158, p. 50-65.

Giles, P.T., 2001. Remote sensing and cast shadows in mountainous terrain. Photogrammetric engineering and remote sensing, v. 67(7), p. 833-840.

Gupta, R., Haritashya, U.K. and Singh, P., 2005. Mapping dry/wet snow cover in the Indian Himalayas using IRS multispectral imagery. Remote sensing of Environment, v. 97(4), p. 458-469.

Hall, D.K., Riggs, G.A. and Salomonson, V.V., 1995. Development of methods for mapping global snow cover using moderate resolution imaging spectroradiometer data. Remote sensing of Environment, v. 54(2), p. 127-140.

Hu, J.M. and Shean, D., 2022. Improving mountain snow and land cover mapping using very-high-resolution (VHR) optical satellite images and random forest machine learning models. Remote Sensing, v. 14(17), https://doi.org/10.3390/rs14174227.

Javanmard, S., Yatagai, A., Nodzu, M., BodaghJamali, J. and Kawamoto, H., 2010. Comparing high-resolution gridded precipitation data with satellite rainfall estimates of TRMM_3B42 over Iran. Advances in Geosciences, v. 25, p. 119-125.

Jia, S., Zhu, W., Lű, A. and Yan, T., 2011. A statistical spatial downscaling algorithm of TRMM precipitation based on NDVI and DEM in the Qaidam Basin of China. Remote sensing of Environment, v. 115(12), p. 3069-3079.

Liu, Y., Lei, Y., Zhang, J., Li, X., Huang, X. and Wang, X., 2021. Spatiotemporal variations of snow cover in the Karakoram Mountains based on MODIS data from 2000 to 2019. International Journal of Digital Earth, v. 14(3), p. 313-328.

Mitterwallner, V., Steinbauer, M., Mathes, G. and Walentowitz, A., 2024. Global reduction of snow cover in ski areas under climate change. PLoS One, v. 19(3), e0299735.

Mitterwallner, V., Steinbauer, M., Mathes, G. and Walentowitz, A., 2024. Global reduction of snow cover in ski areas under climate change. PLoS One, v. 19(3), e0299735.

Nagler, T., Rott, H., Ripper, E., Bippus, G. and Hetzenecker, M., 2016. Advancements for snowmelt monitoring by means of Sentinel-1 SAR. Remote Sensing, v. 8(4), 348 p.

Ortner, G., Michel, A., Spieler, M.B.A., Christen, M., Bühler, Y., Bründl, M. and Bresch, D.N., 2023. Assessing Climate Change Impacts on Snow Avalanche Hazard (Preprint), in review. Cold Regions Science and Technology, https://doi. org/10.2139/ssrn, 4530305, 665 p.

Tekeli, A.E., Akyürek, Z., Şorman, A.A., Şensoy, A. and Şorman, A.Ü., 2005. Using MODIS snow cover maps in modeling snowmelt runoff process in the eastern part of Turkey. Remote sensing of Environment, v. 97(2), p. 216-230.

Varade, D. and Dikshit, O., 2018. Estimation of surface snow wetness using Sentinel-2 multispectral data. ISPRS Annals of the Photogrammetry, Remote Sensing and Spatial Information Sciences, v. 4, p. 223-228.

Willibald, F., Kotlarski, S., Grêt-Regamey, A. and Ludwig, R., 2020. Anthropogenic climate change versus internal climate variability: Impacts on Alpine snow cover. The Cryosphere Discussions, p. 1-23.

Xie, P. and Xiong, A.Y., 2011. A conceptual model for constructing high-resolution gauge-satellite merged precipitation analyses. Journal of Geophysical Research: Atmospheres, 116(D21).

Yan, D., Huang, C., Ma, N. and Zhang, Y., 2020. Improved landsat-based water and snow indices for extracting lake and snow cover/glacier in the tibetan plateau. Water, v. 12(5), 1339 p.

Yarahmadi, M., Azizi, Z. and Khalighi Sigaroudi, S., 2022. Investigating the persistence of snow on vegetation using Landsat 8 images (case study: Erbil province). Journal of Meteorology and Atmospheric Science, v. 5(1), p. 42-52. https://doi.org/10.22034/jmas.2023.380920.1192.